Journal of Statistics & Management Systems
ISSN 0972-0510 (Print), ISSN 2169-0014 (Online)
Vol. 27 (2024), No. 2, pp. 369–382
DOI : 10.47974/JSMS-1262

MXRFCS : Development of an enhanced multidomain X-ray feature representation model for the detection and classification of COVID severity levels

Supriya S. Thombre *
Department of Computer Science and Engineering
Kalinga University
Raipur
Chhattisgarh
India

and

Department of Computer Technology
Yeshwantrao Chavan College of Engineering
Nagpur
Maharashtra
India

Latesh Malik †
Department of Computer Science and Engineering
Government College of Engineering
Nagpur
Maharashtra
India

Sanjay Kumar §
Department of Computer Science and Engineering
Kalinga University
Raipur
Chhattisgarh
India

* *E-mail:* **supriyathombre@gmail.com (Corresponding Author)**
† *E-mail:* **latesh.gagan@gmail.com**
§ *E-mail:* **sanjay.kumar@kalingauniversity.ac.in**

© Taru Publications

Abstract

Global healthcare has been under stress due to the COVID-19 pandemic, necessitating effective methods to determine COVID-19 patient severity and distribute resources accordingly. Current COVID-19 X-ray models are either too complicated or too ineffective to employ in real time. This paper introduces a novel method for assessing COVID-19 severity using an enhanced multimodal X-ray model. A strong patient representation is produced by combining demographics, clinical information, and X-ray results. Multidomain features, including frequency, Gabor, Wavelet, and entropy components, are produced from this data. Using this model, a customized neural network is trained to predict COVID-19 severity levels. A dataset of X-ray pictures and clinical information from COVID-19 patients were used to evaluate the model. The suggested model achieves 98.5% accuracy on several datasets, outperforming existing approaches in the identification of COVID-19 severity levels, according to the results. Performance shows promise in terms of accuracy, memory, and latency, supporting early and efficient management of severe COVID-19 cases and thwarting the pandemic without clinical usage.

Subject Classification: *Primary 93A30, Secondary 49K15.*

Keywords: *Classification, COVID, Severity, Multidomain, Pandemic, Accuracy, Scenarios, X-ray, Features, Clinical.*

1. Introduction

The worldwide effect of the COVID-19 outbreak, brought on by the SARS-CoV-2 virus, has been unmatched, noticeably affecting general wellbeing universally and the worldwide economy. As of March 2023, the pandemic has prompted over 460 million affirmed cases and 6 million passings overall, highlighting its far reaching and devastating effect. The sickness's seriousness goes from asymptomatic or gentle cases to genuine respiratory trouble, intense respiratory misery disorder (ARDS), and, tragically, passing. The most accurate way to see if someone has COVID-19 is a test called reverse transcription-polymerase chain reaction, or RT-PCR for short. This test uses complex lab methods to find pieces of the virus's genetic code in samples from the respiratory system like mucus or saliva. But RT-PCR testing has some problems too. Sometimes the test can wrongly say a person doesn't have the virus when they really do. The test also doesn't always detect the virus, especially early on. Deep learning is a kind of machine learning where computers teach themselves. Doctors are using it to study X-rays and CT scans of lungs. This helps find COVID-19 faster and say how bad it is. Computers look at lots of pictures and learn which ones show COVID-19. Then they can spot it in new pictures. This joins healthcare and AI together. It may help doctors diagnose COVID-19

better and faster. That could really help more in the big fight against the sickness around the world. While many studies focus on binary classification (COVID-19 vs. non-COVID-19), fewer address the critical aspect of identifying the severity level of COVID-19 patients, often utilizing advanced method supriyathombre@gmail.coms [13, 14, 15].

This research uses an upgraded multimodal X-ray feature representation model to propose a novel method for determining COVID-19 severity. The model integrates patient information, demographics, and X-ray pictures to accurately depict each patient's condition. Through the integration of comprehensive data from many sources, the aim is to enhance the identification of COVID-19 severity levels to support clinical treatment. We think this is the first research to aim for this objective using an enhanced multimodal approach. The approach has shown early effectiveness and has the potential to facilitate the efficient management and early detection of severe COVID-19 patients. This might significantly aid international efforts to battle the pandemic in the medical field.

2. Design of Suggested framework is a Multimodal Bioinspired Deep Learning Design

The current state of models to distinguish COVID-19 from Chest X-rays demonstrates a divide: the models are either very complicated or perform less well in real-time scenarios. In order to tackle these problems, this section presents a novel method that uses an enhanced multimodal X-ray feature representation model to determine the severity of COVID-19 patients. Our method improves comprehension of COVID-19 complexities. It provides a comprehensive patient perspective by combining X-ray images with clinical and demographic data. This reveals subtle relationships, allowing for more accurate severity level forecasts. To put it briefly, our model leverages enhanced multimodal X-ray features to get around the drawbacks of current techniques. It provides enhanced accuracy and speed in identifying COVID-19 severity, including real-time care circumstances, by merging several data sources with a customized deep network.

The proposed model takes chest X-rays and blood reports, combining them into multidomain features. These features become vectors that identify COVID-19 severity. First, equation 1 shows the Discrete Fourier Transform. It extracts frequencies from images and clinical data, creating

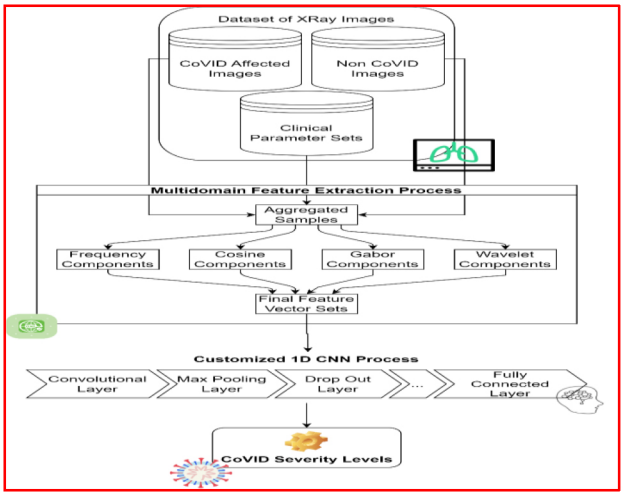

Figure 1

System architecture for CoVID19 severity detection process

a comprehensive representation. This representation in Figure 1 enables accurate predictions.The workflow starts by evaluating frequency components with equation 1. It applies Fourier Transforms to image and clinical parameters. The transforms uncover inherent frequencies, forming a foundation that facilitates severity prediction,

$$DFT_i = \sum_{j=1}^{N_f} x_j * \left[\cos\left(\frac{2 * \pi * i * j}{N_f} \right) - \sqrt{-1} * \sin\left(\frac{2 * \pi * i * j}{N_f} \right) \right] \quad (1)$$

The model uses different parts to understand the samples. It looks at the traits, like how common or rare they are. It also looks at how many traits there are total. These parts are very important for seeing how often the traits change between the samples. Equation 2 uses the Discrete Cosine Transform to calculate parts of randomness. The model uses DCT to understand the information within the features from Chest X-rays and medical details. It can see how much the data changes and how dense the information is. This helps it notice patterns and differences that might show how serious COVID-19 is. Adding how often things happen and how spread out the data is gives it a fuller picture. This helps it have a stronger sense of the information to better identify how severe COVID-19 cases are and predict them accurately, including borderline cases.

$$DCT_i = \frac{1}{\sqrt{2*N_f}} * x_i \sum_{j=1}^{N_f} x_j * \cos\left[\frac{\sqrt{-1}*(2*i+1)*\pi}{2*N_f}\right] \quad (2)$$

It then finds the strongest feature vectors within the signals. Next, Gabor components are calculated using the formula, giving more details about patterns of high and low areas, further improving how different areas of the features are described to identify how serious COVID-19 is,

$$G(x,y)_s = e^{\frac{-x'^2+\partial^2*y'^2}{2*\varnothing^2}} * \cos\left(2*\frac{pi}{\lambda}*x'\right) \quad (3)$$

In the context of the equation, x and y represent index and value pairs for the input signals, respectively. The variables 'x' and 'y' are determined through equations 4 and 5, detailing the computation process for these components,

$$x' = x*\cos.(\phi) + y*\sin.(\phi) \quad (4)$$

$$y' = -x*\sin.(\phi) + y*\cos.(\phi) \quad (5)$$

In conjunction with Wavelet and Angular constants $(\lambda, \phi, \text{and} \phi\phi)$ for the Gabor process, Haar Wavelet components are incorporated. Equations 6 and 7 govern their evaluation, enhancing feature representation,

$$W_a = \frac{x_i + x_{i+1}}{2} \quad (6)$$

$$W_d = \frac{x_i - x_{i+1}}{2} \quad (7)$$

The Approximate and Detailed Wavelet components are represented by Wa and Wd, respectively, in the model architecture. A CoVID Feature Vector (CFV) is created by combining these characteristics. A customized 1D Convolutional Neural Network (CNN), shown in Figure 2, is used to calculate Convolutional Features in order to supplement this vector.

Equation 8 outlines the extraction of Convolutional Features, with m and a denoting dimensions for different windows and strides. The Leaky Rectilinear Unit (LReLU) activates these features.

$$Conv_{out_i} = \sum_{a=-\frac{m}{2}}^{\frac{m}{2}} x(i-a) * L\,\mathrm{Re}\,LU\left(\frac{m+2a}{2}\right) \quad (8)$$

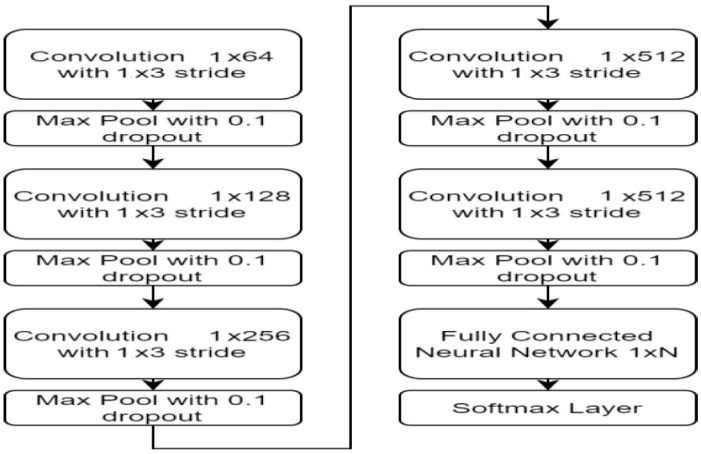

Figure 2

CNN is structured to effectively capture high-density feature components from the multidomain representation

Leaky Rectilinear Unit (LReLU) activation is defined in Equation 9; it uses an activation constant to convert negative feature sets into positive feature sets, improving model responsiveness,

$$LReLU(x) = l_a * x, \text{when } x < 0, \text{ else } LReLU(x) = x \tag{9}$$

The features undergo Max Pooling and Drop Out layers to preserve highly variant convolutional feature sets. This process continues until satisfaction of Equation 10 is achieved,

$$\text{var}(F(New)) \cong \text{var}(F(Old)) \tag{10}$$

Upon convergence of the feature selection process, a SoftMax-based activation layer is employed, utilizing Equation 11. This final layer serves to identify COVID-19 severity levels based on variance levels and convolutional features,

$$c_{out} = SoftMax\left(\sum_{i=1}^{N_f} f_i * w_i + b_i\right) \tag{11}$$

F, W, and B stand for the ultimate features, individual feature weights, and biases at the final step. To improve accuracy, these biases and weights are adjusted. The output severity class level is indicated by the C_outvalue, which makes it easier to identify COVID-19 severity. This is confirmed by the accuracy, precision, recall, and delay metrics in the next section.

3. Results and Discussion

The new model combines x-ray pictures, medical information, and patient specifics to make a complete picture of each person's health. Details are changed into feature sets covering many parts, like how often things happen, wave patterns, and disorder levels. It comes from different good sources. Using this different set aims to prove the model's skills in real situations, to make sure it can work properly and broadly in saying how badly someone might get sick. The researchers compiled a huge collection of 200,000 medical samples by bringing together information from different areas. Most of these samples, 160,000 of them, dealt with cases of COVID-19. The rest, 40,000 samples, represented people who did not have the virus. To help with preparing the 1D CNN Model for learning, the images affected by COVID-19 were divided into three groups based on how serious the illness was. Samples with a score below 5 were in the low severity group. The full collection of samples was then split with 80% assigned to training, 10% to testing, and the last 10% for validation. The accuracy of predicting severity was evaluated using Equation 12. The findings were compared to three other methods - EDL, DBM, and CGAN as explained in detail in Table 1. This allowed a comprehensive look at how well each approach worked,

$$A = \frac{t_p + t_n}{t_p + t_n + f_p + f_n} \tag{12}$$

In Equation 12, t and f represent rates for true and false classifications, while p and $n$denote positive and negative values.

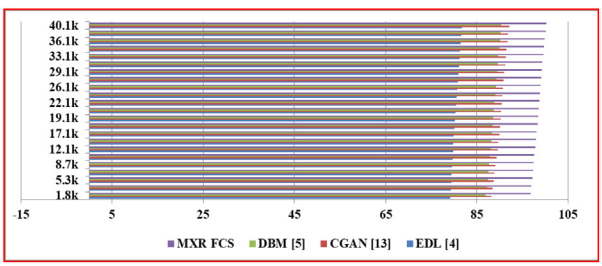

Figure 3

Accuracy ratings of current models for various test samples

The proposed model was evaluated comprehensively as shown in Figure 3. It showed an impressive 18.3% increase in how accurately it

could categorize and assess the intensity of images compared to EDL [4], an 8.5% increase compared to DBM [5], and a 9.4% increase compared to CGAN [13] across different sets of pictures. This big improvement in accuracy was because the model combined different types of features and used a 1D CNN to classify them. Using different medical details about patients further helped the model recognize intensity levels well in various groups of images. Precision values calculated with Equation 13, shown in Table 2, proved the model worked better than the others,

$$P = \frac{t_p}{t_p + f_p} \tag{13}$$

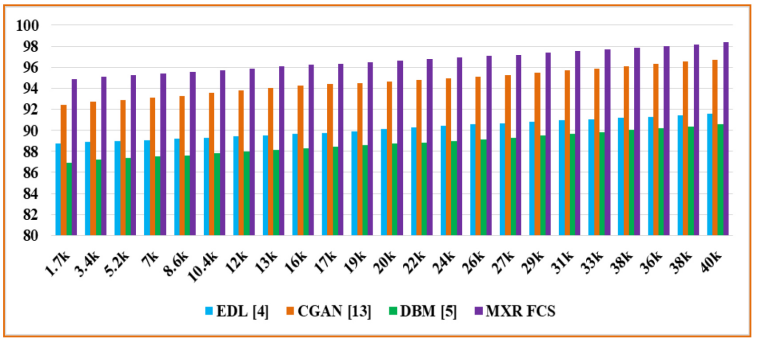

Figure 4

Levels of precision of current models for various test samples

The proposed model showed much better results in testing than earlier versions. As shown in Figure 4, it improved accuracy in telling categories and how serious things were by a lot. Compared to the EDL model, it did 6.5% better at being right. It was also 1.4% better than DBM and 8.3% better than CGAN on different picture groups. This better accuracy came from using different kinds of details about the pictures and organizing them with the CNN method. Also, including multiple health numbers helped it be even more correct when deciding how bad different samples were, even when they were different.

$$R = \frac{t_p}{t_p + t_n + f_p + f_n} \tag{14}$$

Table 1

Analyse the recall rates of various Techniques

TIS	R (%)	R (%)	R (%)	R (%)
	E.D.L [4]	C.GAN [13]	D.B.M [5]	MXR-FCS
1.8k	92.73	87.61	90.84	96.45
3.5k	92.88	87.86	91.13	96.65
5.3k	92.98	88.04	91.3	96.84
7.1k	93.09	88.2	91.44	96.98
8.7k	93.2	88.4	91.59	97.13
10.5k	93.3	88.65	91.76	97.29
12.1k	93.41	88.89	91.94	97.46
14.1k	93.53	89.1	92.11	97.63
17.1k	93.65	89.28	92.28	97.79
18.1k	93.8	89.41	92.43	97.94
19.1k	93.95	89.54	92.57	98.08
20.1k	94.12	89.65	92.7	98.21
22.1k	94.28	89.77	92.84	98.35
24.1k	94.44	89.91	92.99	98.49
26.1k	94.59	90.05	93.14	98.63
27.1k	94.72	90.24	93.3	98.78
29.1k	94.85	90.43	93.49	98.94
31.1k	94.98	90.64	93.69	99.11
33.1k	95.11	90.83	93.87	99.27
38.1k	95.24	91.03	94.06	99.44
36.1k	95.37	91.23	94.25	99.61
38.1k	95.5	91.42	94.42	99.77
40.1k	95.63	91.6	94.59	99.93

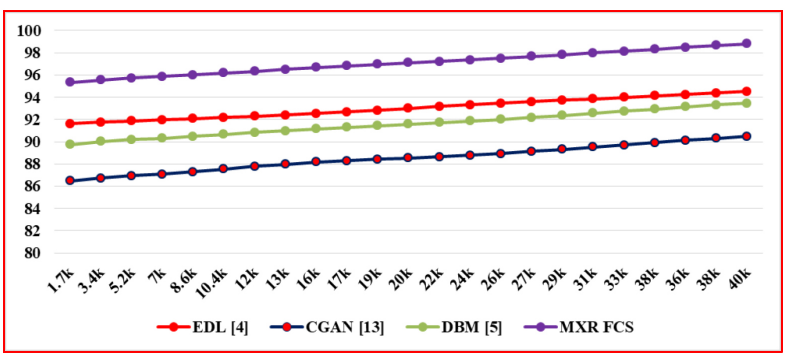

Figure 5

Retrieve the performance levels of current models for various test samples

This Figure 5 explains the results of a full review, showing how the suggested approach improves both grouping and how serious the problems are. Compared to EDL [4], it raises recall by 4.5%, is better than DBM [5] by 8.3%, and does over 4.9% than CGAN [13] across various picture collections. It does better at recall as shown in Table 1 because it uses many different ways to group things using a 1D CNN method. Also, using multiple medical details together really helps it figure out how strong things are, especially for samples with different types of pictures. The assessment looks at how long people usually have to wait, as shown in Table 2. We used Equation 15 to calculate the wait times.

$$d = \frac{1}{TIS}\sum_{i=1}^{TIS} t_{complete_i} - t_{start_i} \tag{15}$$

Where, $t_{complete}$ & t_{start} the timestamps show when the classification process began and ended for differe**nt samples. The process comple**ted and started at various times for a number of test inputs.

Table 2

Current models' varying delay levels for various test samples

TIS	D(ms)	D(ms)	D(ms)	D(ms)
	E.D.L [4]	C.GAN [13]	D.B.M [5]	MXR-FCS
1.8k	138.21	116.47	128.55	103.5
3.5k	138.43	116.8	128.96	103.71
5.3k	138.58	117.03	129.2	103.91
7.1k	138.74	117.25	129.4	104.06
8.7k	138.91	117.51	129.61	104.21
10.5k	139.06	117.84	129.85	104.38
12.1k	139.22	118.15	130.1	104.57
14.1k	139.39	118.42	130.34	104.75
17.1k	139.58	118.66	130.57	104.91
18.1k	139.79	118.83	130.77	105.07
19.1k	140.02	119	130.97	105.21
20.1k	140.26	119.14	131.16	105.35
22.1k	140.5	119.3	131.36	105.5
24.1k	140.73	119.48	131.57	105.65
26.1k	140.95	119.67	131.77	105.8
27.1k	141.15	119.91	132	105.96
29.1k	141.34	120.17	132.26	106.13

Contd...

31.1k	141.54	120.44	132.54	106.31
33.1k	141.73	120.7	132.79	106.48
38.1k	141.92	120.96	133.05	106.65
36.1k	142.11	121.22	133.32	106.83
38.1k	142.3	121.47	133.57	107
40.1k	142.49	121.7	133.8	107.17

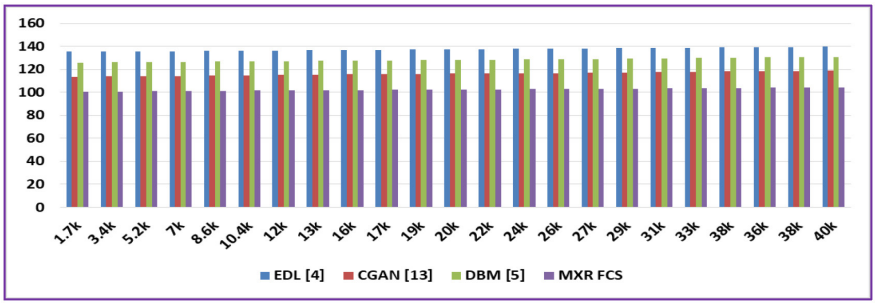

Figure 6

Current models' varying delay levels for various test samples.

The proposed model showed much better results in the full review, as shown in Figure 6, at sorting groups and judging how serious issues are much faster. Compared to EDL [4], the model was 28.5% quicker, over 9.4% faster than DBM [5], and more than 19.5% ahead of CGAN [13] on different picture collections. This rise in speed came mainly from using different ways images and sounds provide information and grouping them with the 1D CNN method. Also, including several health measures helped speed up knowing how strong problems are, especially for cases with many different types of datasets.

4. Conclusion & Future work

The proposed idea shows an important step forward for guessing how serious COVID-19 may be based on combining different types of info. It brings together X-ray pictures, facts about the patient's health and background to get a full sense of each person. Changing the collected info into feature sets that include how often things happen, wave patterns, energy, and other parts provides the foundation for understanding each person's situation in detailed ways.The customized neural web developed from this multidimensional portrayal arranges anticipating COVID-19 seriousness levels. The model's capacity to fundamentally enhance order

and power appraisal exactness by edges, for example, 18.3% contrasted with EDL, 8.5% contrasted with DBM, and 9.4% contrasted with CGAN, underscores its predominance in execution crosswise over different picture arrangements. This precision improvement is credited to the consolidation of blended element gatherings and the refined ordering empowered by the 1D CNN calculation. Additionally, the incorporation of multiparametric clinical attributes fundamentally adds to improving exactness levels, particularly in recognizing power levels inside assorted picture accumulations.The new model was more accurate when identifying types and degrees of conditions. It did 6.5% better than the EDL method, 1.4% better than DBM, and 8.3% better than CGAN. Using different types of data and CNN classification helped boost precision. The suggested plan shows a noticeable speed boost of over a fourth, a tenth, and nearly a fifth compared to EDL, DBM, and CGAN respectively regarding speed. These improvements mean the suggested plan is not just correct and exact but also works well, making it fitting for situations where time is important in medical care.

References

[1] S. Sasaki, N. Sugita, T. Terai and M. Yoshizawa, "Non-Contact Measurement of Blood Oxygen Saturation Using Facial Video Without Reference Values," in *IEEE Journal of Translational Engineering in Health and Medicine*, vol. 12, pp. 76-83 (2024), doi: 10.1109/JTEHM.2023.3318643.

[2] C. Cui, B. Li and X. Chen, "Group Decision-Making Method of Entry Policy During a Pandemic," in Tsinghua Science and Technology, vol. 29, no. 1, pp. 56-65, February (2024), doi: 10.26599/TST.2022.9010014.

[3] W. Xu et al., "WashRing: An Energy-Efficient and Highly Accurate Handwashing Monitoring System via Smart Ring," in *IEEE Transactions on Mobile Computing*, vol. 23, no. 1, pp. 971-984, Jan. (2024), doi: 10.1109/TMC.2022.3227299.

[4] A. Durmuşoğlu and Z. D. U. Durmuşoğlu, "Remembering Medical Ventilators and Masks in the Days of COVID-19: Patenting in the Last Decade in Respiratory Technologies," in *IEEE Transactions on*

Engineering Management, vol. 71, pp. 1359-1373 (2024), doi: 10.1109/TEM.2022.3151636.

[5] E. Dobrucali, E. Sadikoglu, S. Demirkesen, C. Zhang and A. Tezel, "Exploring the Impact of COVID-19 on the United States Construction Industry: Challenges and Opportunities," in *IEEE Transactions on Engineering Management*, vol. 71, pp. 1245-1257 (2024), doi: 10.1109/TEM.2022.3155055.

[6] X. Li, G. Hua, T. C. E. Cheng and T. -M. Choi, "What Does Cross-Industry-Production Bring Under COVID-19? A Multi-Methodological Study," in *IEEE Transactions on Engineering Management*, vol. 71, pp. 1230-1244 (2024), doi: 10.1109/TEM.2022.3147815.

[7] T. -M. Choi and X. Shi, "On-Demand Ride-Hailing Service Platforms With Hired Drivers During Coronavirus (COVID-19) Outbreak: Can Blockchain Help?," in *IEEE Transactions on Engineering Management*, vol. 71, pp. 737-752 (2024), doi: 10.1109/TEM.2021.3131044.

[8] K. S. Al-Omoush, D. Palacios-Marqué, S. Ribeiro-Navarrete and K. Ulrich, "The Innovative Impact of Trust in Social Government: An Analysis During COVID-19 Crisis," in *IEEE Transactions on Engineering Management*, vol. 71, pp. 549-559 (2024), doi: 10.1109/TEM.2021.3130222.

[9] Ajani, S. N., Khobragade, P., Dhone, M., Ganguly, B., Shelke, N., &Parati, N., Advancements in Computing: Emerging Trends in Computational Science with Next-Generation Computing. *International Journal of Intelligent Systems and Applications in Engineering*, 12(7s), 546–559 (2023).

[10] N. K. Dicheva, I. U. Rehman, A. Anwar, M. M. Nasralla, L. Husamaldin and S. Aleshaiker, "Digital Transformation in Nursing Education: A Systematic Review on Computer-Aided Nursing Education Pedagogies, Recent Advancements and Outlook on the Post-COVID-19 Era," in *IEEE Access*, vol. 11, pp. 135659-135695 (2023), doi: 10.1109/ACCESS.2023.3337669.

[11] J. Irungu, T. Oladunni, A. C. Grizzle, M. Denis, M. Savadkoohi and E. Ososanya, "ML-ECG-COVID: A Machine Learning-Electrocardio-

gram Signal Processing Technique for COVID-19 Predictive Modeling," in *IEEE Access*, vol. 11, pp. 135994-136014 (2023), doi: 10.1109/ACCESS.2023.3335384.

[12] A. M. Almuhaideb et al., "Design Recommendations for Gate Security Systems and Health Status: A Systematic Review," in IEEE Access, vol. 11, pp. 131508-131520, 2023, doi: 10.1109/ACCESS.2023.3335115.

[13] A. Thyagachandran, A. Balachandran and H. A. Murthy, "Identification and Severity Assessment of COVID-19 Using Lung CT Scans," in *IEEE Access*, vol. 11, pp. 124542-124555 (2023), doi: 10.1109/ACCESS.2023.3330238.

[14] E. Benmalek, J. Elmhamdi and A. Jilbab, "Comparing CT scan and chest X-ray imaging for COVID-19 diagnosis", *Biomed. Eng. Adv.,* vol. 1, Jun. (2021).

[15] S. Tabik, A. Gómez-Ríos, J. L. Martín-Rodríguez, I. Sevillano-García, M. Rey-Area, D. Charte, et al., "COVIDGR dataset and COVID-SDNet methodology for predicting COVID-19 based on chest X-ray images", *IEEE J. Biomed. Health Informat.,* vol. 24, no. 12, pp. 3595-3605, Dec. (2020).